Inorganica Chimica Acta, 39 (1980) 153–160
©Elsevier Sequoia S.A., Lausanne – Printed in Switzerland

SO_2 Binding to a Metal–Metal Bond: Vibrational Spectra of $Fe_2(CO)_8SO_2$

C. SOURISSEAU and J. CORSET

L.A.S.I.R. - C.N.R.S., 2, rue Henri Dunant, 94320 Thiais, France

Received July 5, 1979

Infrared and Raman spectra (3000–10 cm^{-1}) are reported for $Fe_2(CO)_8SO_2$ in the solid state at 300 and 100 K. An assignment for most of the vibrational modes is proposed. Spectroscopic and X-ray diffraction data concerning the SO_2 bridged molecule are correlated. An approximate valence force field calculation has been performed and the Fe–Fe, Fe–S and $S \cdots O$ bond force constants are estimated equal to 1.12, 1.65 and 7.4 mdyn/Å, respectively: these values are compatible with an electronic donation of SO_2 to the metal–sulfur and metal–metal bonds. The comparison of Raman spectra using different exciting radiations (647.1 nm, 514.5 nm and 488.0 nm) shows that the modes primarily associated with vibrations of the Fe_2S cluster display intensity enhancements by a preresonance Raman effect. The visible absorption at ~480.0 nm is thus assigned to a cluster electronic transition.

Introduction

In order to study the adsorption of small molecules (SO_2, CO_2, CS_2...) on metal surfaces, we have first investigated the vibrational spectra of $Fe_2(CO)_8SO_2$ [1] in which the SO_2 ligand bridges the two groups $Fe(CO)_4$ (Fig. 1). The choice of this very simple model compound is justified by crystallographic data of some trimetallic complexes [2, 3] which show that the SO_2 molecule is coordinated through the sulfur atom bridging only one metal–metal bond.

To our knowledge, only brief reports of the infrared spectrum of this compound are existant and they mainly discuss the bands characteristic of the C≡O and $S \cdots O$ stretching vibrations [4, 5]. We have investigated complete infrared and Raman spectra of the solid complex at 300 K and 100 K in order to assign all vibrational modes and to correlate spectroscopic results with the structure of bridging SO_2. In addition, from a normal coordinate calculation, we have estimated the Fe–Fe, Fe–S and $S \cdots O$ bond strengths. Finally, new information about the nature of the first electronic transition of the compound is obtained from a study of the preresonance Raman spectra.

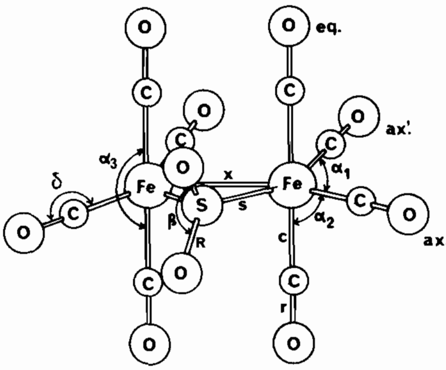

Fig. 1. Structure of $Fe_2(CO)_8SO_2$ (taken from ref. 1) with internal coordinates defined. Molecular parameters: distances Fe–Fe = 2.717 A, Fe–C = 1.800 A, CO = 1.150 A, Fe–S = 2.220 A, SO = 1.45 A; angles $C_{ax}FeC_{ax'}$ = 108.25°, $C_{ax}FeC_{eq}$ = 90.8°, $C_{eq}FeC_{eq}$ = 177°, FeCO = 180°, OSO = 114°.

Experimental

$Fe_2(CO)_8SO_2$ was prepared according Field and Newlands' procedure [5] and recrystallized from CH_2Cl_2 in order to get yellow-orange crystals. The complex decomposes, without melting at 125 °C (lit. 120–125 °C [4]; 100 °C [5]) and its purity was checked by several analyses.

$Fe_2C_8O_{10}S$, calc. (%): Fe, 27.93; C, 24.08; S, 8.02. Found (%): Fe, 27.10; C, 23.60; S, 7.94.

Infrared spectra at room temperature and at liquid nitrogen temperature (~100 K on the sample were obtained from nujol and fluorolube mulls with the Perkin-Elmer 225 and 180 instruments (3000–180 cm^{-1}) and with a Polytec FIR 30 interferometer (310–10 cm^{-1}).

Raman spectra were recorded on a triple monochromator Coderg T 800 instrument with the exciting wavelengths 647.1 nm (Kr^+), 514.5 nm and 488.0 nm (Ar^+) of two Spectra Physics model 164 lasers. Raman spectra at room temperature were obtained using a sample holder rotating at *ca.* 1600 r.p.m. [6, 7] and those at 100 K from $KClO_4$ disks of the sample in conjunction with a glass block

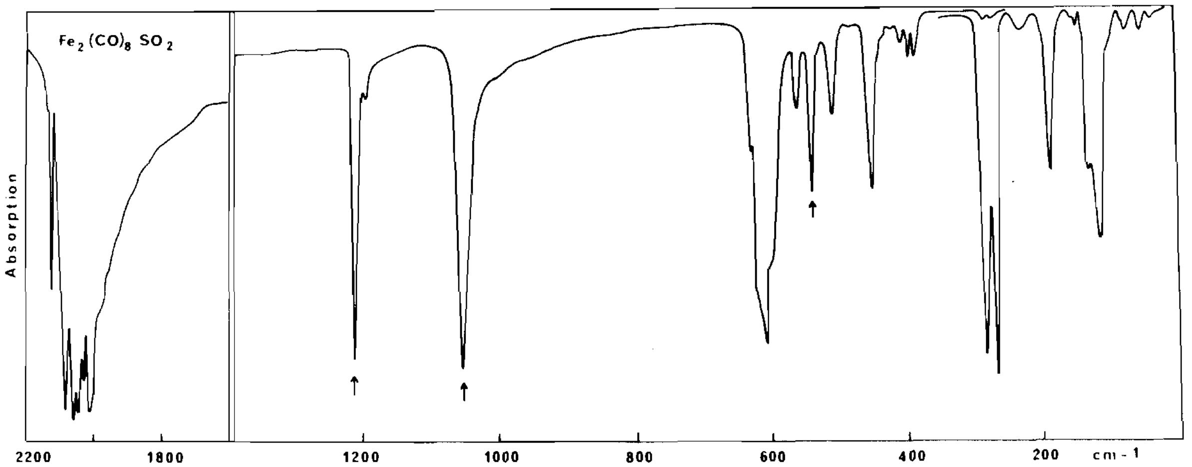

Fig. 2. Infrared spectrum of the $Fe_2(CO)_8SO_2$ solid complex at 300 K. (the arrows indicate bands assigned to the SO_2 internal vibrations).

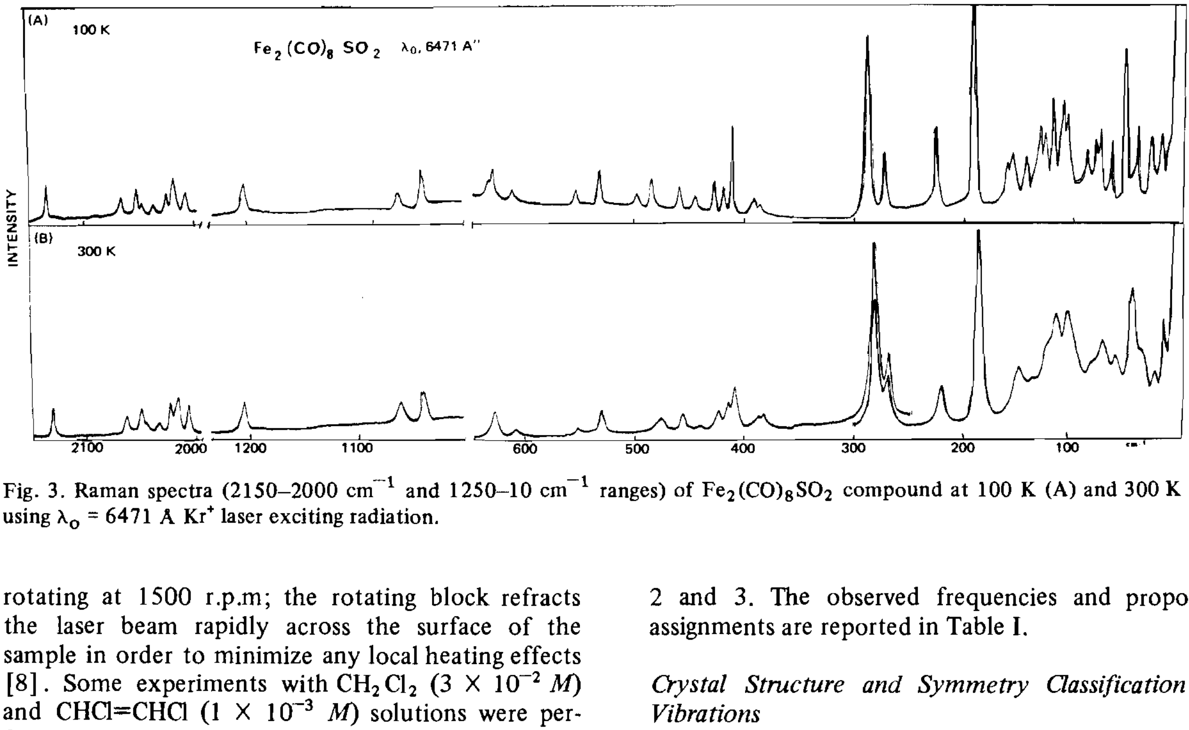

Fig. 3. Raman spectra (2150–2000 cm^{-1} and 1250–10 cm^{-1} ranges) of $Fe_2(CO)_8SO_2$ compound at 100 K (A) and 300 K (B) using λ_0 = 6471 Å Kr^+ laser exciting radiation.

rotating at 1500 r.p.m; the rotating block refracts the laser beam rapidly across the surface of the sample in order to minimize any local heating effects [8]. Some experiments with CH_2Cl_2 (3×10^{-2} *M*) and CHCl=CHCl (1×10^{-3} *M*) solutions were performed using a rotating liquid cell; however, because of the low solubilities and rapid decomposition of solutions under the laser beam, only three bands were observed at 284 and 181 cm^{-1} (polarized) and at 216 cm^{-1} (depolarized).

UV–visible electronic spectra were recorded on a Cary 14 instrument by transmission and diffuse reflectance.

Results and Discussion

Infrared and Raman spectra (2100–10 cm^{-1}) of $Fe_2(CO)_8SO_2$ in the solid state are shown in Figs. 2 and 3. The observed frequencies and proposed assignments are reported in Table I.

Crystal Structure and Symmetry Classification of Vibrations

The compound crystallizes [1] in the monoclinic space group $P2_1/c$ (C_{2h}^5) with four molecules per unit cell. The free complex has effective C_{2v} symmetry and the 57 internal modes are classified as follows:

$$\Gamma_{vib} = 18\,A_1 + 11\,A_2 + 16\,B_1 + 12\,B_2$$

In the solid state, one expects $4 \times 57 = 228$ vibrations ($57\,A_g + 57\,B_g + 57\,A_u + 57\,B_u$) and each mode must give rise to two Raman active components ($A_g + B_g$) plus two infrared active bands (A_u + B_u). In addition, 21 external vibrations ($6\,A_g + 6\,B_g$ +

TABLE I. Infrared and Raman Vibrational Frequencies (cm^{-1}) and Assignments of Normal Modes for $Fe_2(CO)_8SO_2$ in the Solid State.

Infrared[a]				Raman[b]			Assignments
300 K	int.	100 K	int.	300 K	(int)	100 K	
2132	M	2134	M	2132	(5)	2134	νC≡O
2127	vw	2129	vw	–			
–		2094	sh				
2089	vs	2090	vs				
2068	vs	2972	vs				
–		2069	sh	2064	(4)	2066	
2051	vs	2053	vs	2050	(5)	2052	
2039	sh	2040	s	2046	(3)	2047	
2036	s	2037	s	2035	(2)	2037	
2026	sh	2027	sh	2024	(6)	2025	
2020	vs	2022	vs				
2016	vs	2017	vs	2017	(7)	2018	
2010	s	2011	s	2007	(6)	2008	
1992	M	1992	M				
1986	M	1986	M	–			
1978	M	1977	M				
1209	s	1205	s	1203	(5)	1204	$\nu_a\,{}^{32}SO_2$
		1196	sh				
1192	M	1189	M	1188	(1)		$\nu_a\,{}^{34}SO_2$
1181	vw	1180	vw				
		1063	M	1062	(4)	1063	$2 \times \delta SO_2 = 2 \times 530 = 1060$ cm^{-1}
1053	sh	1053	s				
1048	s	1048	s	1048	(6)	1044	$\nu_s\,{}^{32}SO_2$
1040	sh	1039	M				$\nu_s\,{}^{34}SO_2$
1027	vw	1027	vw				
		634	M			632	δFe–CO
629	M	630	M	627	(9)	629	
620	sh	623	s	–			
615	s	619	s				
		609	s				
605	s	605	s	608	(4)	610	
		598	s				
594	M	594	s	–			
551	M	554	M	552	(2)	553	
		546	sh				
530	M	531	s	530	(9)	531	$\delta\,{}^{32}SO_2$
526	sh	527	sh				$\delta\,{}^{34}SO_2$
		503	M				νFe–C
499	M	496	M			499	
–		488	vw	487	(6)	484	
467	vw	472	w				
456	vw	460	w	457	(7)	460	
442	M	445	s	442	(2)	446	
432	sh	436	M				
425	vw	428	vw	424	(8)	427	
414	vw	417	vw	416	(11)	419	
408	vw	410	w	410	(16)	411	
397	w	400	M				
		396	sh				
		390	vw	390	(4)	391	
383	w	386	M	383	(6)	385	

(continued overleaf)

TABLE I. *(continued)*

Infrared[a]				Raman[b]			Assignments
300 K	int.	100 K	int.	300 K	(int)	100 K	
282	w	288	w	284	(65)	289	νs Fe–S
269	w	272	w	271	(25)	273	ν_a Fe–S
225	vw	226	w	222	(23)	227	δ O–S–Fe (wagging SO_2)
188	w	192	w	188	(100)	192	ν Fe–Fe
						162	
152	vw	158	vw	153	(26)	156	
142	vw	145	vw	140	sh	144	δ O–S–Fe (rocking and twisting SO_2)
						132	
127	w	132	w	126	sh	127	+
116	w	117	w	117	(51)	119	
						111	δC–Fe–C
102	vw	103	vw	106	(53)	107	
83	vw	86	vw	86	(24)	88	+
						80	δS–Fe–C + δC–Fe–Fe
77	vw	76	vw	75	(34)	76	
				62	(24)	66	
52	vw	57	vw	46	(61)	54	
				39	sh	43	
35	vw	36	vw	–			Lattice modes
				26	(12)	30	
				18	(40)	21	

[a] Infrared intensities with the symbols: vs = very strong, s = strong, M = medium, w = weak, vw = very weak, sh = shoulder.
[b] Raman intensities are compared with the strongest band at 188 cm^{-1} of intensity (100).

5 A_u + $4B_u$) of the crystal are expected. However, the lattice modes and some internal deformations (δS–Fe–C, δC–Fe–Fe) must appear at frequencies lower than 100 cm^{-1} and their assignment is difficult.

Vibrational Assignments

The C≡O stretching modes for terminal carbonyl groups, expected near 2000 cm^{-1}, are observed in the range 2130–1980 cm^{-1}. All the sixteen expected νC≡O vibrations (Table I) are observed in infrared, while only eight Raman bands are detected. The average frequency of these vibrations, equal to 2046 cm^{-1}, is higher than those of corresponding unsubstituted carbonyl compounds, as for example 2027 cm^{-1} in $Fe_2(CO)_9$ [9] : the SO_2 ligand seems to be a weaker electron donor than bridging carbon monoxide groups. The SO_2 molecule is characterized by the very strong absorptions at 1209 and 1048 cm^{-1} assigned to ν_a and ν_s stretching modes, respectively [10] while the bending vibration is observed at 530 cm^{-1}. The corresponding Raman bands show a weak intensity suggesting a low value for the polarizability derivative of $S \overset{\cdots}{—} O$ bonds. These bonds behave like polar ones, $^{\delta-}S \overset{\cdots}{—} O^{\delta+}$ and a π electronic delocalization must be existant which strengthens internal bonds of the Fe_2S cluster. The observation in the solid state spectrum of four infrared components for ν_a and $\nu_s SO_2$ vibrations can be explained by an isotopic effect of ^{32}S and ^{34}S atoms; their natural abundance is 95% and 4.2% respectively. We have thus estimated the vibrational frequencies equal to 1206, 1048 and 530 cm^{-1} for $^{32}SO_2$ and to 1190, 1049 and 526 cm^{-1} for $^{34}SO_2$ ligand; the theoretical [11] and experimental ratio $(\nu_s \times \delta)^{32}SO_2/(\nu_s \times \delta)^{34}SO_2$ are very close, 1.0303 and 1.0309 respectively.

It is important to notice that the frequency decrease of the S=O stretching modes on going from the free [12] to the complexed state are roughly equal to 150 and 100 cm^{-1} whereas, according to the X-ray data, the variations of S–O distances are quite small, 1.43 Å [13] as compared with 1.45 Å [1]. However, the O–S–O angle (114°) is sensitive to the complex formation since in solid SO_2 this angle is trigonal (119.5°). We have intended to confirm these geometric changes using an approximate calculation on the XY_2 model [11]. Such a calculation performed for both isotopic ligands shows not only a weakening of the S–O bond force constants in the complex but also a slight closure of the O–S–O angle, from 120° to 117.8°. We do not again find the 114° experimental value because, in particular, the anharmonicity of vibrations has not been taken into account [14].

The bands observed in the ranges 640–550 and 500–380 cm^{-1} are assigned by comparison with the spectra of some carbonyl compounds [9, 15–17] to Fe–C–O bending modes and to Fe–C stretching vibrations. Moreover, the strongest Raman bands at 284 and 188 cm^{-1} (polarized) are assigned indoubtedly to ν_sFe–S and νFe–Fe vibrations. As a matter of fact, the former vibration has been observed at near 300 cm^{-1} in $Fe_2(CO)_6(SCH_3)_2$ and in $Fe_2(CO)_6S_2$ compounds while the frequencies of the stretching metal–metal bonds, which are bridged by two sulfur atoms, are equal to 207 and 195 cm^{-1} [15, 16], respectively. A Raman band at 204 cm^{-1} has been recently assigned to this mode with $Fe_2(CO)_6S_2CH_2$ compound [18]. Finally, for $Fe_2(CO)_8^{2-}$ anions which have a direct iron–iron bond, this vibration has been observed near 170 cm^{-1} [19]. So, our reported value (188 cm^{-1}) for a single sulfur bridged metal–metal bond is quite reasonable. However, it is difficult to correlate vibrational frequencies with intermetallic distances because, on one hand, of the vibrational coupling and, on the other hand, of the steric effects of bridging ligands. In the above mentioned systems these bond distances span a rather wide range of values from 2.485 Å in $Fe_2(CO)_6S_2CH_2$ [18] to 2.787 Å in $Fe_2(CO)_8^{2-}$ [20].

The bands observed at 220, 150 and 120 cm^{-1} can be assigned to the wagging, rocking and twisting modes of the SO_2 molecule (δO–S–Fe) and all the bands below 110 cm^{-1} arise from bending vibrations (δC–Fe–C, δS–Fe–C and δC–Fe–fe) and from lattice modes. In this low frequency range, the Raman spectrum at 100 K is well resolved (Fig. 3) and some bands split into two components; nevertheless, the spectra are not markedly different suggesting that no phase transition is existing.

Finally, it is noteworthy that most infrared and Raman components have close frequency values (Table I). Only Van der Waals interactions take place between the molecules as in molecular crystals.

Normal Coordinate Analysis

An approximate normal coordinate analysis was carried out to clarify the nature of the observed normal modes and to estimate Fe–S and Fe–Fe bond force constants. Schachtschneider' programs [21], GMAT, VBN and FPERT were used to construct the G matrix and to solve the secular equations with least-squares adjustment of the force constants [22]. The molecular parameters and internal coordinates are given in Fig. 1. Only the A_1 block was calculated and the C–Fe–S and C–Fe–Fe angle bending coordinates were not taken into account because they contribute mainly to modes at very low frequencies. However, C–Fe–C coordinates have been included in order to estimate their interaction with the Fe–Fe stretching mode. In a first approximation, the nine A_1 modes, 3νC≡O, 3δFeCO and 3νFe–C, were assigned to the strongest Raman bands.

TABLE II. Results of Normal Coordinate Analysis for the A_1 Symmetry Block of $Fe_2(CO)_8SO_2$.

Frequencies, cm^{-1} obsd	Frequencies, cm^{-1} calcd	Potential Energy Distributions % (major contributors)
2132	2132.9	νCO, 94
2050	2050.9	νCO, 94
2017	2017.0	νCO, 94
1041	1042.6	$\nu_s SO_2$, 91
627	641.9	δFe–C–O, 53; νFe–C, 14; δC–Fe–C, 12
608	595.3	δFe–C–O, 87
552	549.8	δFe–C–O, 86
530	532.1	δSO_2, 55; νFe–C, 13; νFe–S, 12
487	490.0	νFe–C, 94
457	452.6	νFe–C, 64; δFe–C–O, 10
410	408.0	νFe–C, 68; νFe–S, 10
284	283.3	νFe–S, 48; νFe–Fe, 23; δSO_2, 15
188	186.9	νFe–Fe, 49; δC–Fe–C, 16; νFe–S, 13
106	104.2	δC–Fe–C, 74
86	85.0	δC–Fe–C, 86
62	56.7	δC–Fe–C, 89

Valence force constants were used to construct the F matrix and off-diagonal elements have been neglected. The principal force constants were estimated from literature values for analogous sytems [16] and were then refined to fit the observed frequencies. Results are given in Tables II and III.

A satisfactory agreement between observed and calculated frequencies has been obtained (Table II). The frequencies which primarly involve motions of the Fe_2S cluster are calculated within experimental accuracy and we note some vibrational coupling of the νFe–S, νFe–Fe and δSO_2 modes. The metal–metal stretching vibration (49% νFe–Fe) shows also an appreciable contribution from C–Fe–C bending modes (16% of potential energy distribution). These δC–Fe–C vibrations have calculated at frequencies lower than 110 cm^{-1} in agreement with the assignments made above. Values of the C≡O, Fe–C, Fe–S stretching force constants and of Fe–C–O, C–Fe–C bending constants (Table III) can be well compared with those proposed by Scovell and Spiro [16] in $Fe_2(CO)_6S_2$. On the other hand, we note some decrease of the metal–metal force constant from 1.3 to 1.1 mdyn/Å in agreement with Badger's empirical rule [23], *i.e.* with the variations of interatomic distances, 2.550 and 2.717 Å respectively. The relatively low value of the S–O stretching constant, 7.4 mdyn/Å as compared to 10.2 mdyn/Å for the free molecule (Table III), is in accordance with our

TABLE III. Adjusted Valence Force Constants for $Fe_2(CO)_8SO_2$ and Comparison with Analogous Compounds.

Int. Coordinate	Force Constants		Average Values	Analogous Compounds [ref.]
r_i	$f(\nu CO)_{ax}$	= 17.4 mdyn/Å	16.33 mdyn/Å	16.20 mdyn/Å in $Fe_2(CO)_6S_2$ [16]
	$f(_\nu CO)_{ax'}$	= 16.1 mdyn/Å		
	$f(_\nu CO)_{eq}$	= 15.5 mdyn/Å		
c_i	$f(_\nu FeC)_{ax\ or\ ax'}$	= 2.6 mdyn/Å	2.70 mdyn/Å	2.59 mdyn/Å in $Fe_2(CO)_6S_2$
	$f(_\nu FeC)_{eq}$	= 2.9 mdyn/Å		
S	$f(_\nu FeS)$	= 1.65 mdyn/Å	–	1.62 mdyn/Å in $Fe_2(CO)_6S_2$
X	$f(_\nu Fe–Fe)$	= 1.12 mdyn/Å	–	1.30 mdyn/Å in $Fe_2(CO)_6S_2$
δ_i	$f(_\delta FeCO)_{ax}$	= 0.95 mdyn × Å/rad	0.80 mdyn × Å/rad	0.87 mdyn × Å/rad in $Fe_2(CO)_6S_2$
	$f(_\delta FeCO)_{ax'}$	= 0.80 mdyn × Å/rad		
	$f(_\delta FeCO)_{eq}$	= 0.65 mdyn × Å/rad		
α_i	$f(_\delta C_{ax}FeC_{ax'})$	= 0.40 mdyn × Å/rad	0.53 mdyn × Å/rad	0.315 mdyn × Å/rad in $Fe_2(CO)_6S_2$
	$f(_\delta C_{ax}FeC_{eq})$	= 0.68 mdyn × Å/rad		
	$f(_\delta C_{eq}FeC_{eq})$	= 0.52 mdyn × Å/rad		
R	$f(_\nu SO_2)$	= 7.4 mdyn/Å	–	10.2 mdyn/Å in SO_2 [12]
β	$f(_\delta SO_2)$	= 1.62 mdyn × Å/rad	–	1.63 mdyn × Å/rad in SO_2 [12]

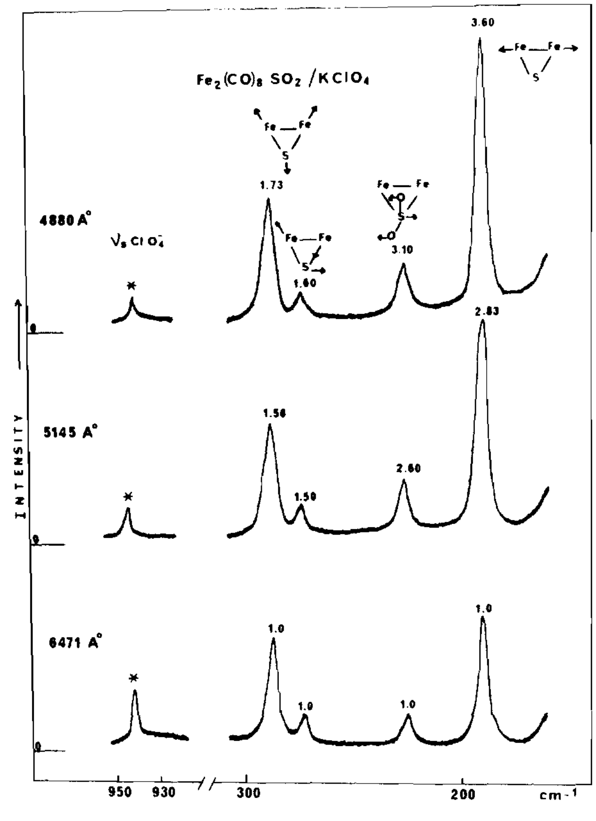

Fig. 4. Raman spectra in the range 300–160 cm^{-1} of Fe_2-$(CO)_8SO_2$ obtained with different laser excitations (6471) 5145 and 4880 Å). The Raman intensities are compared with those of the internal standard (ν_s ClO_4^-) and normalized for each band at 6471 Å. A schematic representation of the corresponding normal modes, ν_sFeS, ν_aFeS, wag. SO_2 and νFe–Fe is given.

interpretation of the spectroscopic results and confirms that SO_2 is a strong electron donor.

However, the O–S–O bending constant value does not display any appreciable change and this may be explained by a cancellation of electronic and geometric factors. In conclusion, the SO_2 binding weakens the S–O bond force constants and strengthens bonds of the Fe_2S cluster.

Raman Intensities

While a rigourous analysis of Raman intensities in solution in order to estimate bond polarizability derivatives is precluded (see experimental part), we have nevertheless obtained new information from the solid state spectra using different exciting radiations. However, the solid complex decomposes rapidly under the laser beam when it is tuned with wavelengths in the range 480.0–350.0 nm. We have only succeeded in getting spectra from pressed disks with $KClO_4$ maintained at ~100 K using low power (≤20 mW) of the radiations 647.1, 514.5 and 488.0 nm. The results in the frequency range 300–160 cm^{-1} are given in Fig. 4. As the maximum of the first electronic transition at about 480.0 nm (Fig. 5) is approached we observe a great intensity enhancement of the bands at 192 and 227 cm^{-1} and also some increase of the bands at 271 and 284 cm^{-1}. The corresponding vibrational modes are concerned mainly with variations of Fe–Fe and Fe–S bond distances and they must be involved in the geometry changes of the complex in the excited state [24]. A similar preresonance enhancement of the bands assigned to the Fe–Fe, Fe–S and S–S stretching vibrations has also been suggested in the Raman

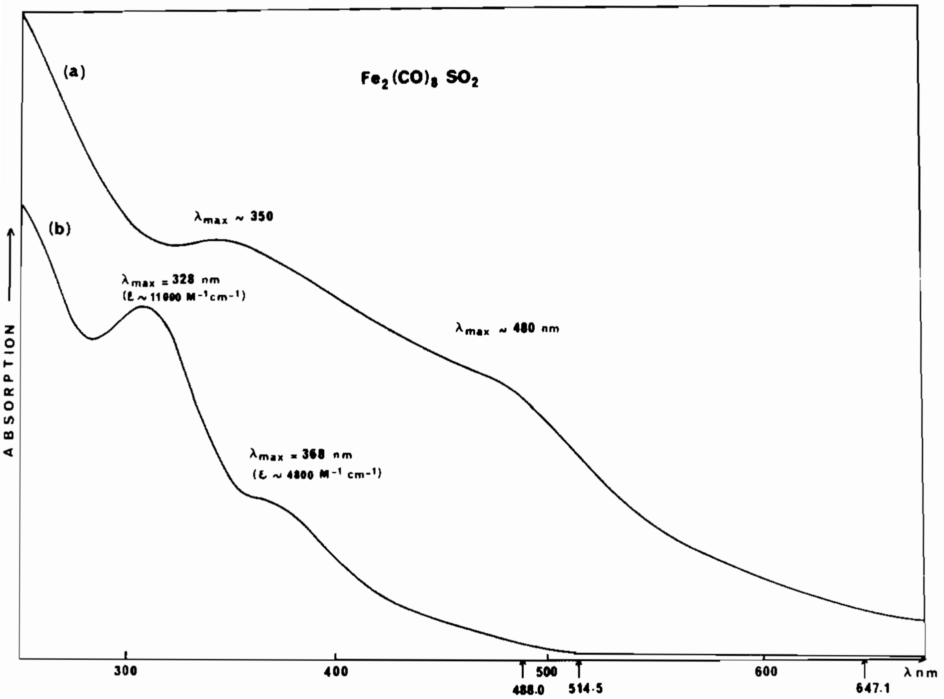

Fig. 5. UV–visible electronic spectra (670–250 nm) of $Fe_2(CO_8)SO_2$ in the solid state (a), obtained by diffuse reflectance and by diluting the solid in the white pigment $MgCO_3$, and of a CH_2Cl_2 solution (b). Both spectra show absorption maxima at different frequencies but the values reported in spectrum a) are only approximate due to the broad bands observed.

spectrum (at λ_o = 676.4 nm) of $Fe_2(CO)_6S_2$; the electronic absorption spectrum of this orange complex shows a broad shoulder at near 470.0 nm. Moreover, we have observed only a weak intensity enhancement for the SO_2 bending vibration and no preresonance effects for the S–O stretching modes. In conclusion, the electronic transition at ~480.0 nm is mainly responsible for the Raman intensity enhancements; this absorption is undoubtedly associated with one Fe_2S cluster transition.

Acknowledgments

We are grateful to J. Hervieu and M. C. Vitorge for technical assistance and we thank D.G.R.S.T. for its financial support by contract nr. 767 11 13.

References

1 J. Meunier-Piret, P. Piret and M. Van Meerssche, *Bull. Soc. Chim. Belges, 76,* 374 (1967).
2 S. Otsuka, Y. Tatsuno, M. Miki, T. Aoki, M. Matsumoto, H. Yoshioka and K. Nakatsu, *Chem. Comm.,* 445 (1973).
3 D. C. Moody and R. R. Ryan, *Inorg. Chem., 16,* 1052 (1977).
4 E. H. Braye and W. Hübel, *Angew. Chem. Internat. Edit., 2,* 217 (1963).
5 D. S. Field and M. J. Newlands, *J. Organomet. Chem., 27,* 221 (1971).
6 R. J. H. Clark, in 'Adv. in Infrared and Raman Spectroscopy', *1,* 143 (1975).
7 W. Kiefer, in 'Adv. in Infrared and Raman Spectroscopy', *3,* 1 (1977).
8 R. J. H. Clark and P. C. Turtle, *Inorg. Chem., 17,* 2526 (1978).
9 I. S. Butler, S. Kishner and K. R. Plowman, *J. Mol. Struct., 43,* 9 (1978).
10 G. J. Kubas, *Inorg. Chem., 18,* 182 (1979) and ref. therein.
11 G. Herzberg, in 'Molecular Spectra and Molecular Structure. II. Infrared and Raman Spectra of Polyatomic Molecules', D. Van Nostrand, N.Y., 169–170 (1962).
12 P. Thirugnanasambandam and S. Mohan, *J. Chem. Phys., 61,* 470 (1974).
13 R. Post, R. S. Schwartz and I. Fankuchen, *Acta Cryst., 5,* 372 (1952).
14 D. Maillard, M. Allavena and J. P. Perchard, *Spectrochim. Acta, Part A, 31,* 1523 (1975).
15 S. F. A. Kettle and P. L. Stanghellini, *Inorg. Chem., 16,* 753 (1977).
16 W. H. Scovell and T. G. Spiro, *Inorg. Chem., 13,* 304 (1974) and ref. therein.
17 D. H. Finseth, C. Sourisseau and F. A. Miller, *J. Phys. Chem., 80,* 1248 (1976).
18 A. Shaver, P. J. Fitzpatrick, K. Steliou and I. S. Butler, *J. Am. Chem. Soc., 101,* 1313 (1979).
19 S. Onaka and D. F. Shriver, *Inorg. Chem., 15,* 915 (1976).

20 H. B. Chin, M. B. Smith, R. D. Wilson and R. Bau, *J. Am. Chem. Soc.*, *96*, 5285 (1974).
21 J. H. Schachtschneider, Technical Reports 231-64 and 57-65, Shell Development Co, Emeryville, Calif., 1964 and 1965.
22 E. B. Wilson Jr, J. D. Decius and P. C. Cross, in 'Molecular Vibrations', McGraw–Hill, N.Y. (1955).
23 R. M. Badger, *J. Chem. Phys.*, *2*, 128 (1934).
24 Y. Nishimura. A. Y. Hirakawa and M. Tsuboi, in 'Adv. in Infrared and Raman Spectroscopy', *5*, 217 (1978).